The role of initial flow conditions for sibilant fricative production (L)

Annemie Van Hirtum[a] and Yo Fujiso
GIPSA-Lab, UMR CNRS 5216, Grenoble University, 11 rue des Mathématiques (BP46), 38402 Grenoble, France

Kazunori Nozaki
Osaka University Dental Hospital, 1-8 Yamadaoka, Suita, Osaka 565-0871, Japan

(Received 26 May 2014; revised 10 October 2014; accepted 16 October 2014)

Sibilant fricative sound production depends on the geometric and flow properties of the production system. Nevertheless, few studies deal with the potential impact of flow properties other than the inlet volume flow rate on the noise produced. In this work, an experimental study is presented using a replica based on a reconstructed oral cavity for the phoneme /s/. Initial flow conditions upstream from the sibilant groove are altered by varying the method of air supply. Statistical moments of the initial velocity distribution are characterized using hot-film anemometry and related to spectral features of the radiated acoustic pressure. Discrepancies in the dynamic amplitude ($\leq$25%) and negative spectral slope ($\leq$35%) observed at a constant Reynolds number but different initial upstream flow conditions are of the same order of magnitude as those previously reported in humans. This suggests that consideration of the upstream flow conditions is important in the study of sibilant fricative sound production. © *2014 Acoustical Society of America*.
[http://dx.doi.org/10.1121/1.4900595]

PACS number(s): 43.70.Jt, 43.70.Aj [ZZ] Pages: 2922–2925

I. INTRODUCTION

The underlying mechanism of sibilant fricative sound production is generally described as noise produced due to the interaction of a turbulent jet, issued from a constriction between the tongue and hard palate—i.e., the sibilant groove—somewhere in the vocal tract, with a downstream wall or obstacle.[1] Screening of geometric and flow parameters during human sibilant fricative phoneme production showed their impact on acoustic features.[2] Nevertheless, flow and geometrical parameters of human sibilant fricative utterances are inherently correlated with each other and show a large inter- and intra-speaker variability.[2,3] To overcome these difficulties proper to human sibilant phoneme data, several studies rely on *ex vivo* data—following experimental, numerical or modeling studies—in order to single out the influence of an individual sibilant production parameter (either geometric or flow) and to perform a systematic study of its impact for sibilant fricative sound production.[1,4–7] The cited studies either do not mention flow conditions upstream from jet formation or suppose laminar upstream flow, whereas from literature focusing on jet development it is known that initial upstream flow conditions will affect jet formation and associated sound sources.[8] Since jet formation is an essential part of sibilant fricative production, it is motivated to reflect on the potential impact of upstream flow conditions on the noise produced within the framework of sibilant fricative production. In order to decorrelate geometric and flow properties, we used a fixed-geometry replica of the vocal tract during a phoneme /s/ utterance. The acoustic outcome produced by the replica is quantified for different upstream flow conditions.

II. METHOD

A. Reconstructed geometry

A cone-beam CT scan (CB MercuRay, 512 slices of 512 pixel × 512 pixel grid with accuracy ±0.1 mm) was made for an adult male subject (Japanese native speaker, normal sitting position) while uttering phoneme /s/ following a "medium" loudness instruction (with a flow rate about 21 l/min). The oral cavity volume and its shape were reconstructed using a marching cube method and an optical modeling machine (SOUP 2 600GS, material TSR-829) with spatial accuracy ±0.1 mm.[9] A three-dimensional plaster model of the reconstructed oral cavity geometry is illustrated in Fig. 1(a). The minimum area of the constricted passage has an hydraulic diameter of 2.1 mm. The inlet of the reconstructed portion has an elliptical shape with hydraulic diameter 13 mm.

A rigid mechanical vocal tract replica [Fig. 1(b)] for sibilant /s/ was obtained by smoothly connecting an upstream circular duct with outlet diameter $D = 8$ mm to the reconstructed geometry with elliptical inlet. The connecting portion was designed to have a length of 30 mm with a divergent angle of about 9 degrees so that the flow remained unstalled.[8] The total length of the mechanical replica was 187 mm which corresponds to the averaged length of the vocal tract of an adult male subject.[1]

B. Flow supply and measurement

In order to vary initial flow conditions at the outlet of the circular duct, airflow was provided to the inlet of the replica in the following three different ways:

[a]Author to whom correspondence should be addressed. Electronic mail: annemie.vanhirtum@grenoble-inp.fr

 0001-4966/2014/136(6)/2922/4/$30.00

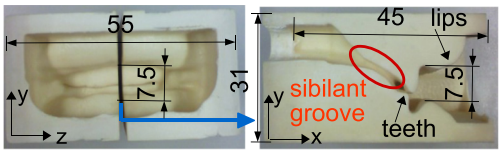

(a)reconstructed oral tract volume: front view and center slice

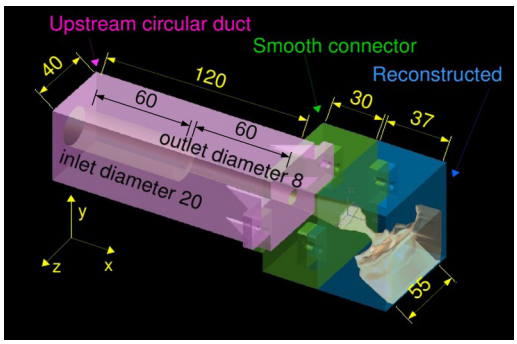

(b)replica of length 187mm in main streamwise direction x

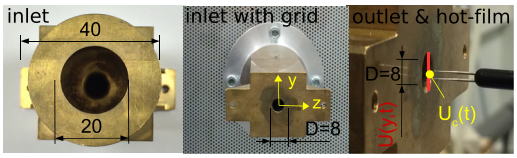

(c)upstream circular duct and initial flow conditioning

FIG. 1. (Color online) (a) Three-dimensional oral cavity reconstruction for the phoneme /s/ [mm]. (b) Schematic overview of the replica [mm]. (c) Upstream circular duct [mm]: inlet, grid at the inlet and hot film at its outlet for initial centerline $U_c(t)$ and transverse $U(y, t)$ velocity profile.

(1) Human (blowing). Airflow was provided to the replica by a human subject blowing at its inlet
(2) Flow facility (no grid). A flow facility was used consisting of an air compressor (Atlas Copco GA7), followed by a pressure regulator (Norgren type 11–818-987) and a manual valve so that the volume flow rate Q was controlled (4043 TSI).[10] The replica was mounted to an upstream settling box ($0.4\,\text{m} \times 0.4\,\text{m} \times 0.5\,\text{m}$) tapered with acoustic foam (SE50-AL-ML Elastomeres Solutions) and equipped with flow straighteners in order to avoid acoustic resonances due to experimental setup upstream from the replica and to homogenize the flow.
(3) Flow facility (grid). The flow facility with settling box was used. A grid (holes of diameter 1.5 mm are spaced 0.8 mm) was inserted between the settling box and the replica [Fig. 1(c)] at the inlet of the upstream circular duct.

In order to characterize initial flow conditions upstream from the reconstructed portion, the flow velocity was measured at the outlet of the circular upstream duct at a streamwise distance $\leq$0.5 mm [Fig. 1(c)] using hot-film anemometry (TSI 1201-20 and IFA 300) and a spatial positioning system (Chuo, 4 μm accuracy).[10] The centerline velocity U_c at $y/D = 0$ was measured as well as the transverse velocity profile for $-0.5 \leq y/D \leq 0.5$ with spatial step $\Delta y/D = 0.11$ for human blowing and $\Delta y/D = 0.038$ for flow facility air supply. At each measurement position, velocity data were sampled at 5 kHz for more than 4 s consecutively for human blowing and 30 s consecutively when the flow facility air supply was used.

Statistical moments[8] of the velocity distribution (local mean velocity U, local turbulence intensity T_u expressing the root mean square of turbulent energy, skewness S_u expressing asymmetry of the distribution due to intermittency and flatness F_u expressing the tail extent of the distribution away from its mean value) at each spatial position were quantified as a function of centerline velocity Reynolds number $Re_c = U_c D/\nu$, with kinematic viscosity of air $\nu = 1.5 \times 10^{-5}\,\text{m}^2/\text{s}$.

C. Acoustic measurement

Acoustic measurements of the noise produced by airflow through the replica were done by inserting the outlet of the replica into a quasi-anechoic chamber (Fig. 2).[11] The quasianechoic chamber was equipped with a pressure-field microphone (B&K 4192, sampling frequency 44.1 kHz) located in the horizontal (xz) plane at an angle of 37°. Based on fricative studies involving human speakers,[2] in our human blowing condition, one was instructed to supply air in three different levels: Soft, medium, and loud. The volume flow rate associated with each instruction was obtained using the volume flow meter (TSI 4000 series) positioned upstream from the settling box and by integration of the transverse mean velocity profile. An overview of instructions and flow conditions is given in Table I. When air was supplied using the flow facility, the volume flow rate was varied so that the associated Reynolds numbers Re_c was within the range relevant for human blowing (Table I) and fricative sibilant production.[2,3]

The acoustic spectra L_p were obtained as the energy normalized sound pressure level (SPL) of the Welch averaged Power Spectral Density[2] $P(f)$,

$$L_p(f) \approx 10 \log_{10}\left(\frac{|P(f)|}{p_{ref}^2}\right), \tag{1}$$

with $p_{ref} = 2 \times 10^{-5}\,\text{Pa}$ and physical frequency f. Concretely, the time-averaging of the periodiograms was performed using Hamming windowed energy normalized time

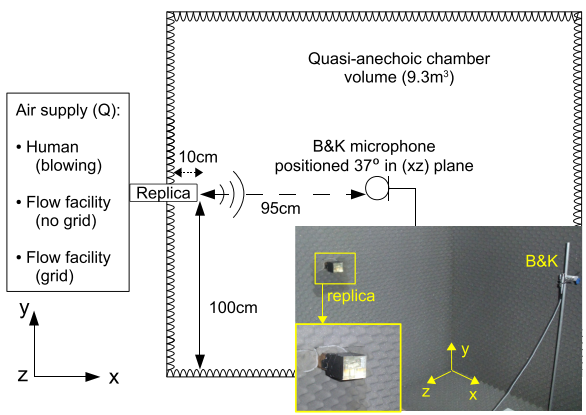

FIG. 2. (Color online) Overview of acoustic measurement setup.

TABLE I. Summary of flow conditions for human blowing during acoustic measurements: instruction and corresponding volume flow rate Q and Reynolds number Re_c.

Instruction	Q [l/min]	Re_c [-]
Soft	11	2850
Medium	21	5250
Loud	45	8850

segments of fixed duration (6 ms) with 50% overlap. The sound pressure spectra were parameterized by considering dynamic amplitude A_d, spectral peak frequency f_m and linear regression slopes S_1 ($f_{min} \leq f \leq f_m$, with f_{min} the frequency associated with minimum spectral amplitude, positive slope) and S_2 ($f_m \leq f \leq 20$ kHz, negative slope) in accordance with fricative spectral characterization.[2]

III. RESULTS

A. Upstream flow characterization

Initial upstream flow conditions are evaluated from initial velocity profiles gathered at the outlet of the circular duct [Fig. 1(c)]. Transverse velocity profiles $U(y)$ from the duct center ($y/D = 0$) up to the duct wall ($y/D = 0.5$) are illustrated in Fig. 3. Normalized mean transverse velocity profiles U/U_c [Fig. 3(a)] are characterized by a uniform ($U/U_c > 0.9$) core region ($|y/D| < 0.3$). The normalized mean velocity within the boundary layer enveloping the core region is observed to increase with increasing Re_c. Therefore, the measured mean velocity profiles approximate top-hat velocity profiles for which the boundary layer displacement thickness depends on Reynolds number[8] and not pipe flows (either laminar or turbulent) for which the boundary layer displacement thickness is not affected by Reynolds number [Fig. 3(a)]. The corresponding transverse profiles of the turbulence intensity [Fig. 3(b)] depend on the Reynolds number Re_c (discrepancy in centerline turbulence intensity $\Delta T_{u,c} \geq 2\%$) and the method of air supply (discrepancy in centerline turbulence intensity $\Delta T_{u,c} \geq 4\%$) for all transverse positions. From the profiles at conditions of $Re_c \leq 1800$ it is observed that turbulence intensities obtained from human blowing are greater than those obtained for air supplied with the flow facility for all values of y/D. In order to characterize initial flow conditions in more detail, statistical moments of the center velocity U_c at $y/D = 0$ [Fig. 1(c)] are shown in Fig. 4 for $500 < Re_c < 15\,000$ and different flow supplies outlined in Sec. II B. The centerline turbulence intensity $T_{u,c}$ [Fig. 4(a)] is affected by the flow supply for all assessed Re_c. Indeed, $T_{u,c} > 3\%$ holds for human blowing which exceeds values observed for flow supplied by the flow facility ($T_{u,c} \leq 3.2\%$). Increasing Re_c increases $T_{u,c}$ regardless of the flow supply (in contrast with what is observed for pipe flow[8]). Nevertheless, transition from a laminar ($T_{u,c} < 0.5\%$) to a turbulent flow regime is observed for flow supplied by the flow facility and not for human blowing. The use of an inlet grid favors turbulence development since first the range of Reynolds numbers for which transition occurs is decreased (from $Re_{u,c} \approx 7000$ to $Re_{u,c} \approx 2000$) and second the turbulence intensity in the transition and turbulent regime is increased ($T_{u,c} \leq 2\%$ without grid and $T_{u,c} \leq 3.2\%$ with grid). Skewness $S_{u,c}$ [Fig. 4(b)] and flatness $F_{u,c}$ [Fig. 4(c)] of the center velocity distribution as a function of Reynolds number further illustrates the impact of the flow supply on initial flow conditions. Indeed, values associated with a Gaussian velocity distribution ($S_{u,c} = 0$ and $F_{u,c} = 3$) provide an approximation for human blowing whereas they provide a poor description for airflow supplied by the flow facility. The deflection from Gaussian values is the most prominent within the transition regime for which the turbulence intensity is mainly due to intermittency and vortex passage and not to random velocity fluctuations characterizing established turbulence with a Gaussian distribution.

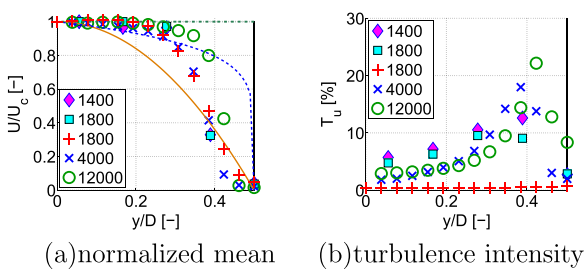

(a)normalized mean (b)turbulence intensity

FIG. 3. (Color online) Illustration of transverse velocity profiles as a function of Reynolds number Re_c and the method of flow supply: Human blowing (◇, □) and flow facility (grid) (+, ×, ○). (a) normalized mean velocity U/U_c (symbols) and developed laminar (full line–parabolic) and turbulent (dashed line–power-law) pipe flows, (b) local turbulence intensity T_u.

B. Acoustic characterization

In order to search the influence of the variation of initial flow conditions on the radiated noise outcome, spectral parameters (dynamic amplitude A_d, spectral peak frequency f_m and spectral slopes $S_{1,2}$) are quantified (Fig. 5). In general, it is observed that spectral parameters depend on Reynolds number

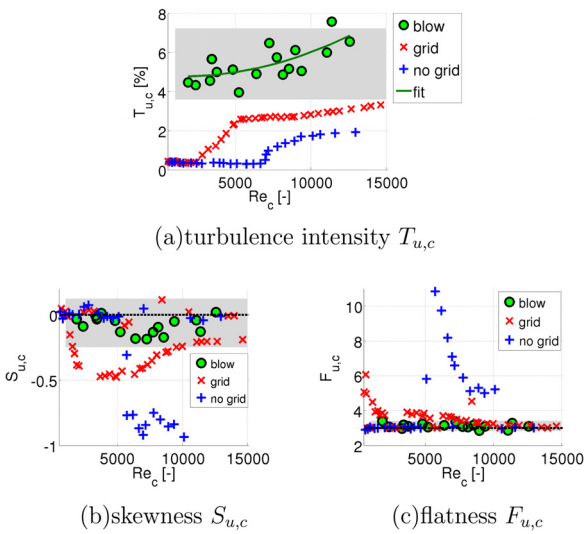

(a)turbulence intensity $T_{u,c}$

(b)skewness $S_{u,c}$ (c)flatness $F_{u,c}$

FIG. 4. (Color online) Centerline initial velocity statistical features as a function of Reynolds number Re_c and the method of flow supply [human blowing (filled ○), flow facility with (×) and without (+) inlet grid]. The gray shaded area indicates the feature range covering 95% of the values observed for human blowing: (a) centerline turbulence intensity $T_{u,c}$ and a quadratic fit (full line) of $T_{u,c}(Re_c)$ (co-efficient of determination $R^2 = 0.6$), (b) skewness $S_{u,c}$ (dashed line $S_{u,c} = 0$), and (c) flatness $F_{u,c}$ (dashed line $F_{u,c} = 3$).

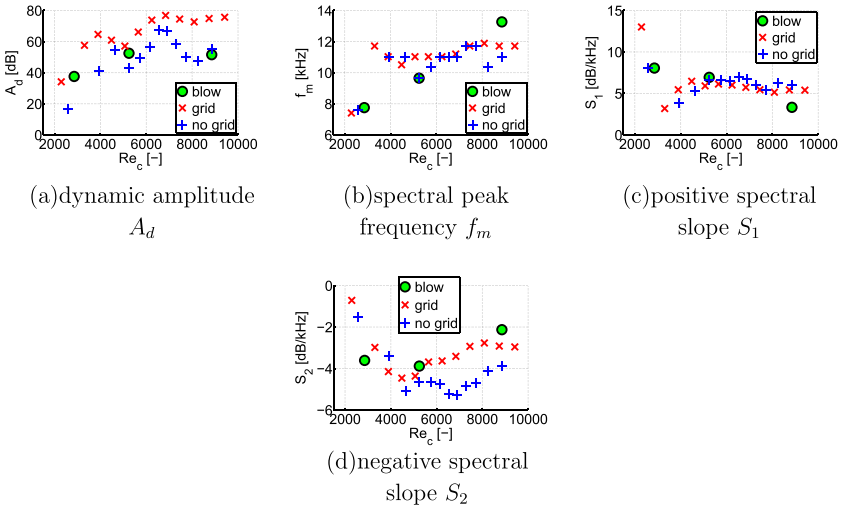

(a)dynamic amplitude A_d (b)spectral peak frequency f_m (c)positive spectral slope S_1 (d)negative spectral slope S_2

FIG. 5. (Color online) Parameters of acoustic spectra as a function of Reynolds number Re_c and the method of flow supply [human blowing (filled ○), flow facility with (×) and without (+) inlet grid].

Re_c and that their order of magnitude does not depend on the method of air supply. Differences are also observed across different air supplies, demonstrating the impact of the variation of initial flow condition outlined in Sec. III A. Indeed, parameters of acoustic spectra obtained using the flow facility alternatively decrease and increase with the Reynolds number Re_c whereas for human blowing current data suggest that spectral parameters are either continuously decreasing (S_1) or increasing (A_d, f_m, and S_2) with the Reynolds number. Obviously, for human blowing theses results need to be confirmed in future due to the limited number of flow conditions (=3, see Table I). Nevertheless, current findings suggest that the evolution of spectral parameters with Re_c reflects the complexity of the flow dynamics as quantified by the statistical centerline velocity moments in Fig. 4, i.e., a developed turbulent flow with a quasi Gaussian velocity distribution and increasing turbulence intensity with increasing Reynolds number for human blowing and complex flow dynamics with a non-Gaussian velocity distribution associated with the transition from a laminar to a turbulent flow regime for flow provided by the flow facility. This statement is further supported by spectral parameters obtained for flow supplied by the flow facility with and without inlet grid. The dynamic amplitude A_d [Fig. 5(a)] for Reynolds numbers in the range $Re_c \approx 7000$ remains almost unaffected by the Reynolds number when a grid is used (difference $<5\%$) whereas it decreases with increasing Reynolds number in absence of a grid (up to a difference of $\approx 25\%$). The influence of the upstream initial velocity distribution for $Re_c \approx 7000$ is also apparent for S_2 [Fig. 5(d)] which is smaller without than with the inlet grid ($\approx 35\%$). Although spectral parameters are generally related, the impact of initial conditions is less notable for S_1 [Fig. 5(d)] and f_m [Fig. 5(b)] than for A_d or S_2. It is noted that the observed differences in acoustic measures for sounds produced with different flow supply methods are of the same order of magnitude or even larger than typical variability observed in human speakers.[2]

IV. CONCLUSION

Noise produced by flow through a reconstructed and rigid replica of the vocal tract during phoneme /s/ is analyzed as a function of the Reynolds number and initial flow conditions by varying the flow supply method. It is shown that at a constant Reynolds number, changes in initial flow properties upstream from the sibilant groove can produce changes in the spectral parameters of the sibilant fricative noise comparable to typical variations observed in human speakers. This is an important finding since initial flow conditions are generally not considered in physical speech production studies. The current experimental results suggest that initial conditions need to be quantified and encourages further research with respect to the impact of the velocity distribution and flow phenomena on the noise source. Further study is needed to account for potential perceptual consequences of the variation of sound properties and to confirm acoustic features for human blowing.

ACKNOWLEDGMENTS

This research was partly supported by JST-ANR grant (PETAFLOW ANR-09-BLAN-0376-01) and by EU-FET grant (EUNISON 308874).

[1]C. Shadle, "The acoustics of fricative consonants," Ph.D. thesis, Massachusetts Institute of Technology, Cambridge, MA (1985), 194 pp.
[2]L. Jesus and C. Shadle, "A parametric study of the spectral characteristics of European Portuguese fricatives," J. Phonetics **30**, 437–464 (2002).
[3]S. Narayanan, A. Alwan, and K. Haker, "An articulatory study of fricative consonants using magnetic resonance imaging," J. Acoust. Soc. Am. **98**, 1325–1347 (1995).
[4]M. Howe and R. McGowan, "Aeroacoustics of [s]," Proc. R. Soc. A **461**, 1005–1028 (2005).
[5]A. Van Hirtum, X. Pelorson, O. Estienne, and H. Bailliet, "Experimental validation of flow models for a rigid vocal tract replica," J. Acoust. Soc. Am. **130**, 2128–2138 (2011).
[6]K. Nozaki, M. Nakamura, H. Takimoto, and S. Wada, "Effect of expiratory flow rate on the acoustic characteristics of sibilant /s/," J. Comput. Sci. **3**, 298–305 (2012).
[7]J. Cisonni, K. Nozaki, A. Van Hirtum, X. Grandchamp, and S. Wada, "Numerical simulation of the influence of the orifice aperture on the flow around a teeth-shaped obstacle," Fluid Dyn. Res. **45**, 1–19 (2013).
[8]S. Pope, *Turbulent Flows* (Cambridge University Press, Cambridge, UK, 2005), 771 pp.
[9]K. Nozaki, "Numerical simulation of sibilant [s] using the real geometry of a human vocal tract," in *High Performance Computing on Vector Systems* (Springer, Germany, 2010), pp. 137–148.
[10]X. Grandchamp, A. Van Hirtum, and X. Pelorson, "Hot film/wire calibration for low to moderate flow velocities," Meas. Sci. Technol. **21**, 1–5 (2010).
[11]A. Van Hirtum and Y. Fujiso, "Insulation room for aero-acoustic experiments at moderate Reynolds and low Mach numbers," Appl. Acoust. **73**, 72–77 (2012).